IJSES
International Journal of Scientific Engineering and Science
Volume 4, Issue 2, pp. 40-47, 2020. ISSN (Online): 2456-7361

Damage Detection in Concrete Using Synthetic Aperture Focusing Technique

Jean Bosco Havugarurema[1], Samson Hansen Sackey[2], Pascal Nkurunziza[3], Emmanuel Nsegiyumva[4]
[1, 2]Department of Internet of Things, Hohai University, Changzhou campus, China, Jiangsu
[3,4]Department of Electrical and Electronic Engineering, University of Rwanda
Email address: [1]hajebocson@gmail.com, [2]3085788751@qq.com, [3]nkupas88@gmail.com, [4]nsengem@gmail.com

Abstract— *The detection of embedded objects inside the concrete has been of great importance to insure the durability. Ultrasonic reconstruction using synthetic aperture focusing technique (SAFT) allow to image the internal structure of concrete and its algorithm focuses ultrasonic signals received at aperture point by coherent superposition that provide a high-resolution image of the region of interest.*

Using SAFT, the representation of concrete volume can be reconstructed with great details, allowing detecting and localizing objects inside the concrete such as construction elements, damage of built-in components or flaws. The inhomogeneous structure of the concrete that lead to disturbing phenomena of the transmitted signal such as attenuation and structural noise are diminished using SAFT. Lab experiments show the behaviors of the elastic wave propagation in the concrete medium and the analysis has been carried out by using COMSOL multi-physics software. The time travel associated with acoustic wave propagation has been analyzed to tune COMSOL in order to detect objects inside the concrete. The results show that the elastic wave based scanning system incorporated with SAFT exhibit high potential in inspecting damage inside the concrete structure.

Keywords— *Ultrasonic wave propagation, synthetic aperture focusing technique, ultrasonic testing, damage detection.*

I. INTRODUCTION

There are many ways the concrete or built-in objects can be damaged and this may cause many problems when the concrete is used without detecting its abnormalities. Ultrasonic nondestructive evaluation technique has been used for long time in testing concrete elements for their quality and safety assurance. For measurement, the point- source/point-receiver is suitable for on-site inspection of civil infrastructures [1]. For applications such as small flaws or tendon ducts detections, the transmission technique suffers from the lack of sensitivity caused by the strongly inhomogeneous structure of the concrete. Strong scattering and structural noise attenuates the transmitted pulses. In order to overcome this problem, signals of low frequencies are used (in the range of 20-100kHz) but the sensitivity of detection of the targeted objects also decreases as the ultrasonic wavelength is of the same magnitude as the embedded aggregate and pores at low frequency. In addition, a wide divergence angle is caused by a low ratio of transducer diameter to wavelength; it also makes the embedded objects not detectable. Sensitive low-bandwidth transducers used for transmission technique have long impulse responses; this makes it not suitable for pulse-echo technique. In order to provide a good way to reduce structural noise by applying pulse echo technique, it is necessary to use transducers of sufficiently short impulse responses [2].

To improve the performance of ultrasonic testing, we have used synthetic aperture focusing technique (SAFT) that provides a constructive interference procedure that enhances the lateral spatial resolution and signal-to-noise ratio. Reconstruction by SAFT offers a general solution as its algorithm numerically superimposes pulse-echo signals measured at several positions, thus creating a high-resolution image [3].

The reminder of the paper is organized as follows. In Section 2, a brief review on ultrasonic wave propagation in concrete from related work is provided. Section 3 gives detailed descriptions of the proposed full condition assessment methodology. In Section 4, we describe the experiments in detail with presentation evaluation results and section 5 concludes our paper with future recommendation.

II. ULTRASONIC WAVE PROPAGATION IN CONCRETE

A. Pulse-echo Transmission

This technique consists of generating an ultrasonic pulse-echo by using an ultrasonic instrument and a transducer [17]. The transducer is placed on the concrete to detect inside objects. The pulse generated travels into the concrete as compressional C- and shear S-waves, and along the surface as Rayleigh wave. Compressional and shear waves propagate into the concrete as spherical wave wave-fronts and are reflected either when they meet internal objects or external boundaries of the concrete. Compressional wave is of great importance in materials testing because its displacement is much faster than the other waves. The C-wave velocity inside concrete material depends on Young's modulus, mass density and Poisson's ratio of the concrete sample and it is calculated as follows:

$$V_C = \sqrt{\left[\frac{E(1-v)}{\rho(1+v)(1-2v)}\right]} \quad (1)$$

Where E represents Young's modulus, ρ stands for mass density and v for Poisson's ratio of concrete

B. Scattering and Structural Noise

Scattering and reflection are two phenomena that occur between two materials of different elastic properties. If the difference in the acoustic impedance is as large as that of

International Journal of Scientific Engineering and Science
Volume 4, Issue 2, pp. 40-47, 2020. ISSN (Online): 2456-7361

concrete to air, most of energy is reflected and no energy is transmitted [2]. An ultrasonic pulse is also scattered by the concrete itself because of its inhomogeneous structure often called structural noise when received as a superposition of many reflections in the received signal as highlighted in Figure 2.1.

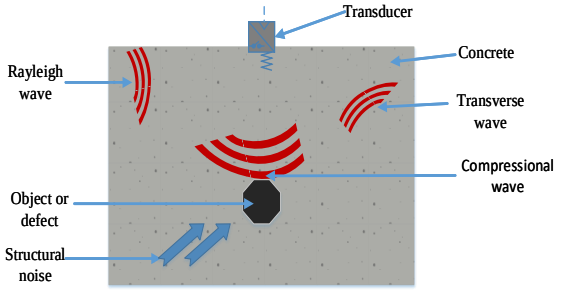

Figure 2.1. Effects of ultrasonic pulse-echo when applied to concrete.

C. Mode Conversion

By considering only the first interaction between the generated elastic field and the defect, figure 2. 3 show that four different waves arrivals are observed at various on the surface [5]. When compressional and shear waves are generated, each of them undergoes mode conversion due to reflection which are C-C (compressional to compressional), C-S (compressional to shear), S-C (shear to compressional) and S-S (shear to shear). As C-wave is faster than S-wave, the first arrival is always C-C. When relying on the geometric distance travelled by the compressional wave from the source to the defect and from the defect to the receiver, the resulting waveform becomes a template defect response. The cross-correlation $f_i(t)$ between the signal $v_i(t)$ at the *i*-th receiver and the reference defect response is defined as follows:

$$f_i(\tau) = \int_{-\infty}^{\infty} v_i(t)\, f_{def}(t+\tau)dt \tag{2}$$

And as result we get f_{def} waveform as the template scatterer response.

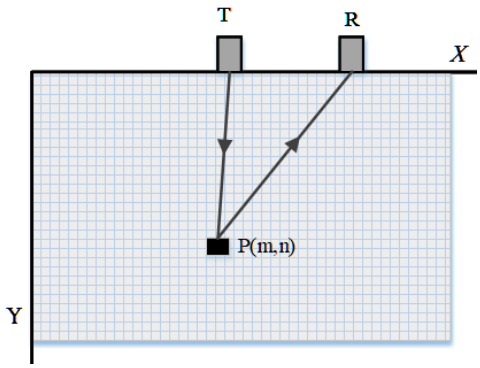

Figure 2.2. Transmission and reception operations for a meshed specimen of concrete

By taking the pixel (m,n) as potential defect as in Figure 2.2, the time travel $T_i^{C\text{-}C}$ of the C-C wave from the source to the pixel and back to the *i*-th receiver is obtained as

$$T_i^{C-C} = \frac{|r_{tp(m,n)}| + |r_{p(m,n)r}|}{V_c} \tag{3}$$

Here $r_{tp(m,n)}$ and $r_{p(m,n)r}$ represent the vectors between the transmitter *(t)* and pixel position *(p)* and the pixel *(p)* and the receiver position *(r)*. And V_c is the compressional wave velocity in the medium.

An associated image value *I(m,n)* related to the chosen pixel is calculated as follow:

$$I^{C-C}(m,n) = \frac{\sum_{i=1}^{N} f_i(T_i^{C-C})}{N} \tag{4}$$

With *N* representing the number of receivers. The image value represents an accumulated effect of the scattered signal from the chosen pixel but based on the wavelets received from various receiver locations.

When considering both compressional (C), shear (S) wave and their mode conversions waves which are C-S, S-C and S-S due to scattering, all can be used combined to generate a high-quality image of the interior of the concrete or other medium. The time of travel and the calculated image value for C-S, S-C and S-S can be computed as follows [5]:

$$T_i^{C-S} = \frac{|r_{tp(m,n)}|}{V_c} + \frac{|r_{p(m,n)r}|}{V_S} \tag{5}$$

$$I^{C-S}(m,n) = \frac{\sum_{i=1}^{N} f_i(T_i^{C-S})}{N} \tag{6}$$

$$T_i^{S-C} = \frac{|r_{tp(m,n)}|}{V_S} + \frac{|r_{p(m,n)r}|}{V_C} \tag{7}$$

$$I^{S-C}(m,n) = \frac{\sum_{i=1}^{N} f_i(T_i^{S-C})}{N} \tag{8}$$

$$T_i^{S-S} = \frac{|r_{tp(m,n)}| + |r_{p(m,n)r}|}{V_S} \tag{9}$$

$$I^{S-S}(m,n) = \frac{\sum_{i=1}^{N} f_i(T_i^{S-S})}{N} \tag{10}$$

And finally, a combined image value is computed as

$$I(m,n) = \left| \frac{\sum_{i=1}^{N} f_i(T_i^{C-C}) + \sum_{i=1}^{N} f_i(T_i^{C-S}) + \sum_{i=1}^{N} f_i(T_i^{S-C}) + \sum_{i=1}^{N} f_i(T_i^{S-S})}{N} \right| \tag{11}$$

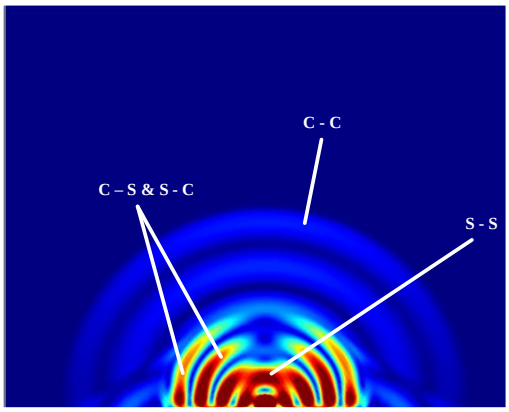

Figure 2.3. Scattered field at the surface of the receiver

International Journal of Scientific Engineering and Science
Volume 4, Issue 2, pp. 40-47, 2020. ISSN (Online): 2456-7361

III. Damage Detection in Concrete Structures

It has been a difficult task to detect internal damages in concrete structures as these abnormalities are not observable at the surface and have the potential to expand and increase the concrete damage when they are not detected for the structure replacement or being repaired. Improvements in technology for doing tests in concrete structures allowed for collection of repeatable and spatially diverse wave impulse time-histories. Many methods have been used, but each technique is known to improve ultrasound image qualities, by its own strengths and drawbacks [23].

A. Basic Concepts of Ultrasonic Detection

Traditionally, Impact-Echo (IE) was an improved, effective and low costly method in evaluating suspected damages in concrete structures but its failure was that it used a very low frequency. This technique is the basic principle where a stress impulse is introduced into the concrete by using a hammer, ball drop, or other impact source, which is monitored by an ultrasonic transducer on the surface [4]. The frequency content of the generated pulse is a function of contact time that must affect the size of the defect to be detected. By using IE, it is possible to detect defects near to the surface, because as the contact time decreases, the frequency content of the pulse becomes more broad-band at a higher center frequency [22]. During the propagation of the pulse generated by the impact source, it is reflected by the internal defects and the time it takes the compressional waves to propagate from the impact source to the defects and come back to the receiver at the surface is

$$t = \frac{2d}{v_c} \tag{12}$$

Where t is the transmit time, d is the distance from the source to the receiver and V_c is the velocity of compressional wave. So, by knowing these parameters it is easy to locate the defect.

B. Detection by Ultrasonic Pulse Velocity Method

This technique is widely used to detect internal defects in concrete structures by estimating the crack depth, compressive strength and other abnormalities [21]. This is the method that uses two transducers attached to the surface of the concrete, as transmitter and receiver. The transmit time and wave velocity are measured. The propagation of ultrasonic waves in concrete is influenced by several parameters such us the type and density of reinforcement, the material composition, severity and location of internal defects, mechanical properties and the surface condition. This makes the transmitted stress waves undergo partial loss and scattering noise due to reflections as discussed [17]. UPV method is based on forward-scattered diffraction of ultrasonic wave at the tips of discontinuity, and it relies on directly reflected signals from the internal structures. So, in order to scan the entire volume, the transducers of broad beam are used so that the entire area with defects will be flooded with ultrasound [23].

As all elastic wave methods, UPV is also a NDT that involves measuring the speed of sound in concrete in order to give details information on the condition of the concrete, and in this method, it is preferable to use longitudinal or compression wave based on their earlier arrival of time. From the Figure 3.1 we can see clearly that the edges of the defect are determined from the difference in time between the lateral waves and the pulses following the paths, P_1 and $P_2(t_1)$, then P_3 and $P_4(t_2)$.

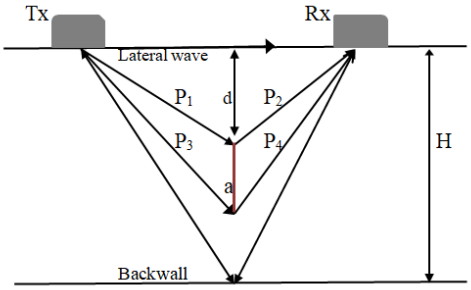

Figure 3.1. Diagram explaining the system signal paths

From the above figure, the following equations are useful in order to know the details about the damage only when the defect is at normal incidence to the surface and if the defect is centrally positioned between the two transducers.

Time to the top of defect, path P_1 and P_2

$$t_1 = \frac{2\sqrt{S^2 + d^2}}{C} \tag{13}$$

Time to the bottom of the defect, path P_3 and P_4

$$t_2 = \frac{2\sqrt{S^2 + (d+a)^2}}{C} \tag{14}$$

Time from the back wall

$$t_{bw} = \frac{2\sqrt{S^2 + H^2}}{C} \tag{15}$$

Where
a = the size of the defect
d= the depth of the defect below the surface
H= Material thickness
C= the longitudinal or compressional wave velocity
S= half of the distance between the two transducers

Note that if the two transducers are close to each other so that the distance between them can be neglected, the equation used to calculate t_1 becomes the basic equation from IE.

Based on the geometry of the figure 3.1 and from the other known parameters, the depth of the defect below the surface (d) and the size of the defect can be calculated as follow:

$$d = \frac{1}{2}\sqrt{C^2 t_1^2 - 4S^2} \tag{16}$$

$$a = \frac{1}{2}\sqrt{C^2 t_2^2 - 4S^2} - d \tag{17}$$

This method has many advantages compared to IE as it gives the accurate value on the depth sizing and it highlights that the height of the defect can be determined.

An exception to this method is that it is not suitable when detecting or sizing defects lying parallel to the surface of inspection. Another advantage is that the diffraction waves are low in amplitude compared to the direct reflection waves and

International Journal of Scientific Engineering and Science
Volume 4, Issue 2, pp. 40-47, 2020. ISSN (Online): 2456-7361

for that reason the sensitivity to damage identification is correspondingly lower in amplitude [24].

C. Synthetic Aperture Focusing Technique in Damage Detection

In the field of damage testing in concrete, synthetic aperture focusing technique was developed to improve the insufficient lateral resolution of reflected ultrasonic pulse-echo data. As concrete is heterogeneous at large scale, ultrasound is scattered and present structure noise in the signal. Most of the time, the implementations of SAFT are performed using a delay-and-sum (DAS) processing in time-domain. Our target is to highlight the advantages of SAFT in NDT application in order to investigate its performance in inspection of damages in concrete structure.

a. SAFT algorithm

In order to illustrate the SAFT principle with a simple model, we consider the measurement setup in the Figure 3.2, which is known in radar applications as a broadside strip-map mode synthetic aperture imaging system. This means that the SAFT system maintains its transducer beam at a broadside during all the period of data acquisition.

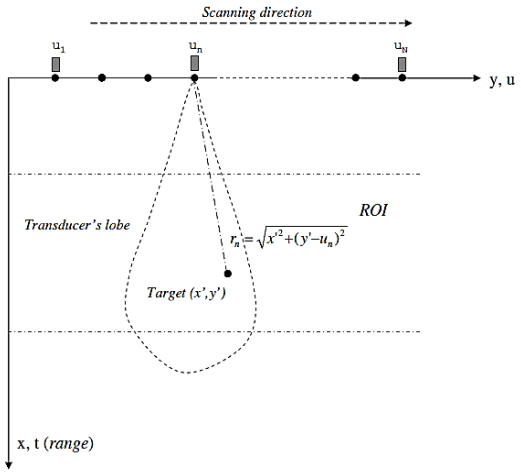

Figure 3.2. Geometry graph for FAST explanation

Here, the region of interest (ROI) may contain any number of reflecting targets (damages which may be flaws or voids...) in the spatial (*x, y*) domain, where *x* is the range while *y* is the cross range. The transducer element moves along the *u* axis, which is parallel to the *y* axis of the target are by transmitting a broadband pulse.

If we consider the transducer's radiation pattern as omnidirectional, then the measured reflected signal at the transducer position u_n will be calculated as [17]

$$e(t,u_n) \approx \iint_{x\ y} f(x,y)\, b(t,x,y-u_n) *_t p\left(t-\frac{2}{c}\sqrt{x^2+(y-u_n)^2}\right) dxdy \quad (18)$$

Where *b (t, x, y)* is the spatial-temporal response of the combined transmitter and receiver apertures and *t means the convolution in time domain. In order for us to achieve focus at an observation point (x', y') in the ROI, the SAFT time-shifts and performs a summation of the received signals e (t,u_n) measured at transducer positions u_n for all *n* in synthetic aperture.

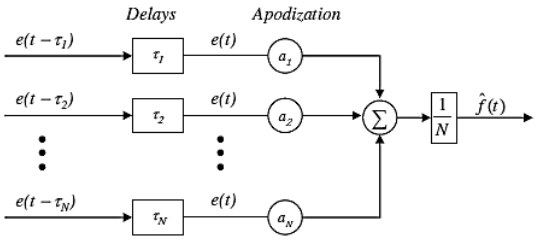

Assuming the point source is valid; the DAS scheme of a time domain SAFT can be highlighted by the block diagram in Figure.3.3. The time delay τ_n aims to compensate for different pulse traveling time and is expressed as

$$\tau_n = \frac{2}{c}(r_n - x') = \frac{2}{c}\left(\sqrt{x'^2 + (y' - u_n)^2} - x'\right)$$

Where *n*=1, 2, 3 …*N* and *N* is the number of element position, r_n is the distance from the element at position u_n to the observation point. A smooth apodization a_n, also known as windowing in spectral analysis, is a single method to control the side lobe levels. After time shifts and summation, the final image is

$$i(x', y') = \sum_{n=0}^{L-1} \frac{a_n e(t - \frac{x'}{c}, u_n)\delta(t-\tau_n)}{r_n} \quad (19)$$

Here the factor $r_n = \sqrt{x'^2 + (y' - u_n)^2}$ is due to the propagation attenuation.

The conventional DAS, used in fixed array focus phased arrays, a certain range *R*, which is the distance from the middle of the ROI to the transducer scanning direction, it needs to be specified in order to determine the delay factor [$\tau_1, \tau_2, \tau_3, \ldots\ldots \tau_N$].

$$\tau_1 = \frac{2}{c}\left(\sqrt{R^2 + (u_1 - y')^2} - R\right) \quad (20)$$

$$\tau_2 = \frac{2}{c}\left(\sqrt{R^2 + (u_2 - y')^2} - R\right) \quad (21)$$

$$\tau_3 = \frac{2}{c}\left(\sqrt{R^2 + (u_3 - y')^2} - R\right) \quad (22)$$

. . .

$$\tau_N = \frac{2}{c}\left(\sqrt{R^2 + (u_N - y')^2} - R\right) \quad (23)$$

Here we can see from Figure 3.1 that y' is the y-coordinate of a target. However, SAFT provides all-depth dynamic focusing effect that enables achieving uniform cross-range resolution in the region of interest. The delay factor applied to the ultrasonic signals at different transducer position must be updated for each range in the region of interest as follows:

$$\tau_{1i} = \frac{2}{c}\left(\sqrt{x'^2 + (u_1 - y')^2} - x_i'\right) \quad (24)$$

International Journal of Scientific Engineering and Science
Volume 4, Issue 2, pp. 40-47, 2020. ISSN (Online): 2456-7361

$$\tau_{2i} = \frac{2}{c}(\sqrt{x'^2 + (u_2 - y')^2} - x_i') \quad (25)$$

$$\tau_{3i} = \frac{2}{c}(\sqrt{x'^2 + (u_3 - y')^2} - x_i') \quad (26)$$

. . .

$$\tau_{Ni} = \frac{2}{c}(\sqrt{x'^2 + (u_N - y')^2} - x_i') \quad (27)$$

Where y' and x_i' are the coordinates of targets from Figure 3.1 Note, that the focusing is performed for all target depths x_i' in ROI, which results in all-depth focusing.

IV. System Model and Results Analysis

Computer simulation has become an essential part in the field of science and engineering but this is a translation of real-world physical laws into virtual form [13], this makes a computer simulation ideal. Nowadays engineers and scientists are using COMSOL Multiphysics software to analyze and simulate designs as in the environment of the real world.

COMSOL Multiphysics is a simulation platform that encompasses all the steps in the modeling workflow: from defining geometries, material properties and the physics that describe specific phenomena for solving and post-processing models for producing accurate and trustworthy results. COMSOL user interface provides a complete simulation environment and a consistent modeling workflow from start until to finish, without regarding the type of design or process being analyzed or developed.

In the basics modules offered by COMSOL Multiphysics, it also includes Acoustics, solid mechanics module, and other physic modeled by a system of PDEs [13]. In this paper, solid mechanics have been used in order to investigate the propagation of acoustic wave in its time dependent domain. The main process is to establish the appropriate geometry model, the physical site definitions (including the materials to be used), set the parameters for the domain and boundary conditions. Once this is well done, it is easy to analyze the results after the signal has been processed.

A. Model Design and Materials

For us to simplify the model we have chosen our geometry to be in 2D instead of 3D in order to avoid complex and longtime calculations. Consider a concrete block specimen with a size of 200mm x 160 mm, the concrete contains a rectangular defect of size 30mm x 3mm as it is shown on Figure 4.1.

The defect is located inside the concrete structure as void, at 100mm and 120mm as abscissa and ordinate respectively. As it can be seen from the figure 4.1, there T1-T16 and R1-R16 that are transmitting and receiving transducers. The first pair of transducers is located at (75, 0) and the last one at (145, 0) on the abscissa which is the scanning direction. Each pair of transducers forms a transmitting and receiving combination, and the distance between them is short so that I can be ignored. The distance between the first measuring point and the following has been modelled to be 5mm during the whole scanning process. During this simulation, the transmitting transducer is set as boundary load that emit a high power single pulse signal as excitation signal with sampling frequency of 0.5MHz.

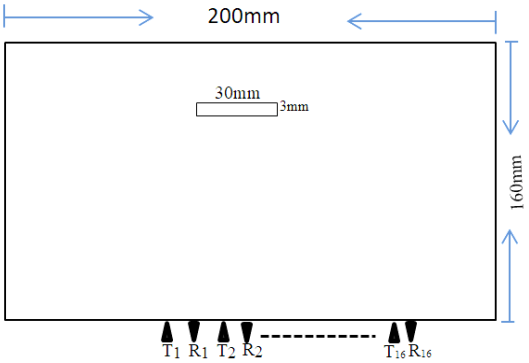

Figure 4.1. Designed model of concrete block specimen with a defect for numerical simulation.

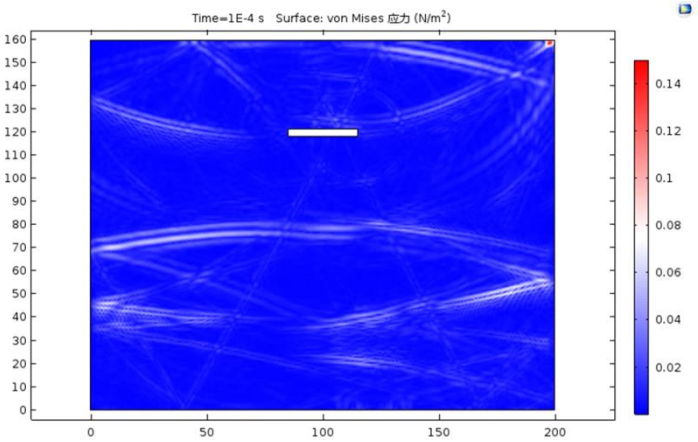

Figure 4.2. Simulation results

The Figure 4.2 shows the simulation results of the designed model. In this result, we can see the meeting results of the waves generated and the results of their behaviors during the propagation process. The excitation source was located at (85, 0) in Cartesian coordinates and this figure provides a visual final response after 1 x 10^{-4} s of simulation.

B. Analysis of Experimental Data

a. 2D simulation analysis

From the Figure 4.3 (a) below, we can see first waves generated after 8.3 µs the after a short period of time, we highlight the transmitted signals in figure 4.3 (b) and figure 4.4(c) which shows as the compressional or longitudinal and shear or transverse waves after 16.65µs and 25 µs as discussed in the previous chapter.

As we will be considering only compressional wave for our further analysis, From Figure 4.3 (b) and Figure 4.4 (c), we can see clearly both compressional and shear waves and identify them as we know that the compression (the first with highest speed) is faster than the shear wave.

Figure 4.4 (d) shows its reflection after meeting the defect at 33.3µs. In addition, the defect reflective wave can also be clearly observed from the same figure.

International Journal of Scientific Engineering and Science
Volume 4, Issue 2, pp. 40-47, 2020. ISSN (Online): 2456-7361

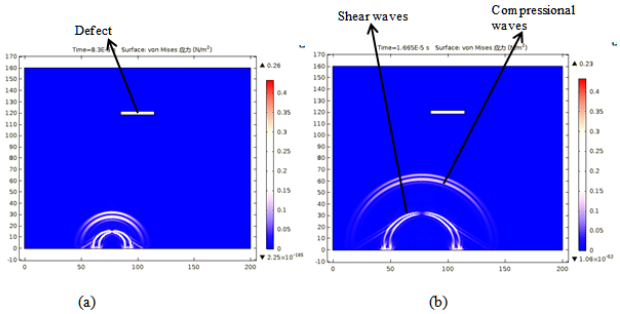

Figure 4.3. Compression and shear wave's highlights.

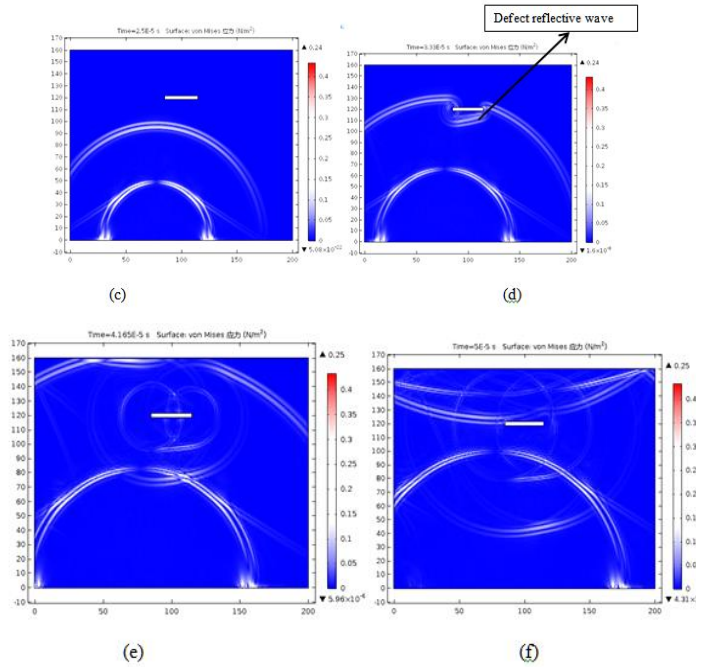

Figure 4.4. Illustration of compressional wave reflection by defect.

Figure 4.5 is the simulation results of all process for duration of 1x 10^{-4} s; from this figure we can notice the following points:

- The ultrasonic radiation is not perfect, this is due to many phenomena such as scattering, structural noise, interference and reflections as discussed.
- From the Figure, it is not easy to identify clearly the defective reflection anymore because of the weakness of the reflective wave from the defect.

b. Simulation analysis of 1D results of the simulated model

From the simulated model, we can easily investigate 1D signals produced by each source chosen when scanning the specimen for the whole process. The figure 4.6 (a) shows us 1D signal results when the source is at (75, 0) which is starting scanning point of our experiment. The figure has 1x10^{-4} s on horizontal axis coordinates, which is the propagation duration from the source to the back-wall, and the figure presents 1 x 10^{-11}mm at its vertical axis as the observation point.

As results of a solid elastic medium such as concrete, when ultrasound wave propagate in it, it produces the deformation by quality points, which in turn become vibrations as the wave passes to the objects or other particles such as defects or damages. So, the figure 4.4 represents the quality point of ultrasound and the resulting displacement as a function of time.

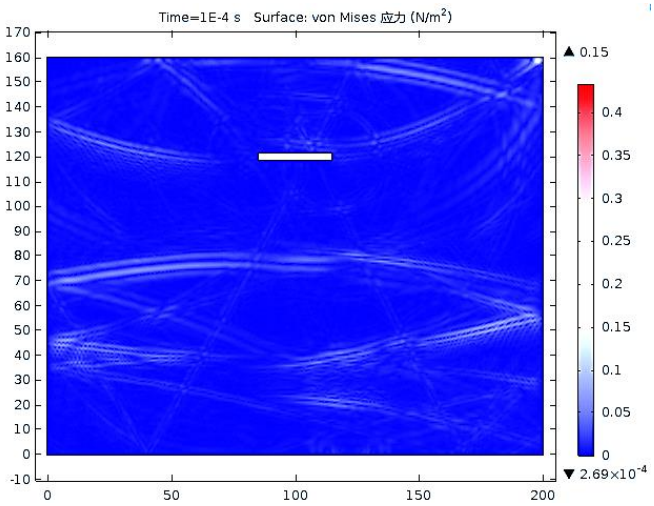

Figure 4.5. Chart analysis of the surface drawing results.

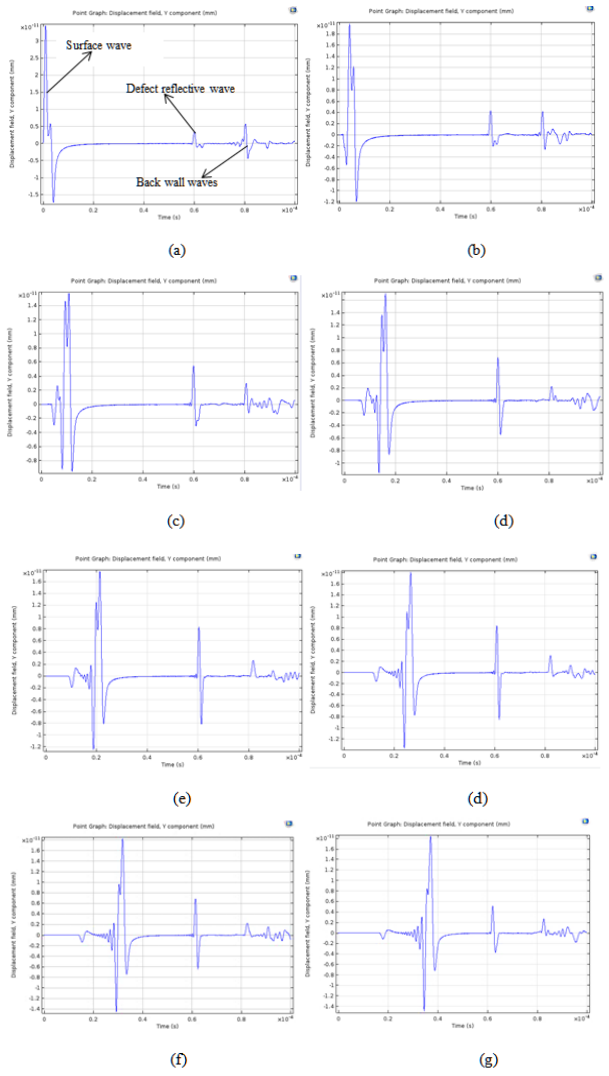

Figure 4.6. Analysis of A-scan graphs at various transmit/receive transducers position.

International Journal of Scientific Engineering and Science
Volume 4, Issue 2, pp. 40-47, 2020. ISSN (Online): 2456-7361

From the figure we can identify the surface wave, defective reflective wave and the back wall reflective wave. It is noted that there is a change in the position of the surface wave as the emitting transducer changes the position as it can be seen from the position (75, 0) of Figure 4.6 (a) to Figure 4.6 (g). This is due to the transducer transmitting angle which means nothing during the detection process.

Moreover, we saw the geometry in the previous chapter, Figure 3.1 that explains clearly this phenomenon, where we have P1 and P3, P2 and P4 as defective reflective waves, and then we have the last one which is the back wall reflective wave. In concrete, the average velocity of propagation is a fixed value, based on the large vibration in function of time, it is easy to calculate at every time the distance between the source emitting signal to the defect or any other damage that causes that kind of large vibration which results in reflecting the emitted wave by using the same basic formula as follow:

$$d = \frac{V_c t}{2} \tag{28}$$

Where V_c, is the compressional wave velocity and t the traveling time from the source to the reflector and back to the receiver.

The main purpose of 1D signal analysis is to figure out the reflections from known or unknown objects or other reflections of the object under consideration. Signal that are expected to be seen are reflections from back wall, reflections from defects and reflections from the boundaries of the object under test. These signals can only help in performing the location estimation of the damage or other useful objects in the concrete once the velocity of the signal is known, but it is a difficult work as it is not easy to differentiate reflection types in 1D signal. Therefore, the values that can be calculated at this step using the basic formulas cannot be trustful.

So, after developing all the seriteria in other to increase the confidence level of damage location, the advanced technique is required.

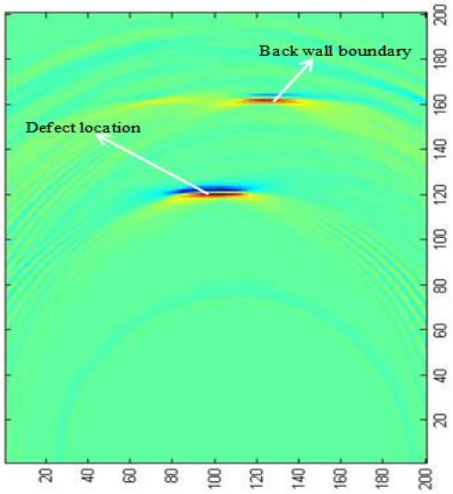

Figure 4.7. SAFT image representing the defect location

C. Data Analysis of the Synthetic Aperture Algorithms

In order to perform SAFT algorithm by using the transducers movement, a group of 8 Transmit/Receive transducer is arranged on the horizontal axis from (75, 0) to (145, 0) coordinates and the distance between them is 5mm. As SAFT algorithm requires so many data for a better performance, in our experiments we used 8 dual transducers by each sending signal and other receive which gave us 64 different data type.

From the above Figure 4.7, after processing data obtained from experiment, it is clearly and easy to identify the location of the defect with open eyes exactly at the same depth position at 120 mm as it was designed in our model sketch of Figure 4.1, because the defect appears as a bright spot. This is due to the fact that SAFT involves an averaging of the scattered field at various receiver positions by suppressing the cluster noise due to the aggregate scattering.

It has been shown that the best performance of the array was achieved using synthetic aperture focusing method in which the generated beam is focused at every point in the target region. This technique also allows the image to be extended beyond the edge of the array whilst still allowing the beam to be focused. This is a significant improvement from swept aperture plane and focused B-scans whose viewable area is dependent on the number of elements used in the aperture. The algorithms were tested using experimental and simulated data and convincing clearly results was obtained.

V. Conclusions and Future Work Recommendations

A. Conclusion

Concrete structures are the mixture of different type of media; it is not an easy task to detect damages inside by using ultrasonic signals because as the elastic waves propagate in concrete are affected by various different interfaces.

As discussed in this work, some phenomena such as reflection, refraction, scattering, structural noise and many more bring difficulties to damage detection process. Sometimes many other built-in objects are imbedded in concrete for other useful reasons, this makes concrete testing more complex because of the presence of more interfaces that make the internal structure of concrete more changed. So, when ultrasonic signals are used to test concrete structures, echo signals are more accurate in other to investigate the reflection signals from different interfaces within the tested specimen. Therefore, in order to improve the ultrasonic inspection system of defects inside concrete structure, we have to analyze all defective reflection waves.

In this work, so many books and papers has been read to gather necessary information on ultrasonic signal and propagation process for better understanding, through a series of theoretical analysis, we were able to design a model using COMSOL Multiphysics software. We studied the propagation process of ultrasonic waves in concrete specimen containing a defect by using COMSOL Multiphysics software and analyze the simulation. Results of this simulation, data obtained have studied and processed to verify the ultrasonic reflection used in this subject. Then, the mathematical model of synthetic aperture focusing algorithm has been applied and verified by MATLAB programming.

- The analysis and process done in this work with theoretical and simulation results, highlight that the method used in this paper has a potential ability for damage or defects detection in concrete structure.

B. Future work

Although synthetic aperture focusing technique has been actively used recently as potential nondestructive method, but here, we list some suggestions for the future research which extend the work of this research:

In this research we only took into consideration compressional or longitudinal waves but as we saw in the principle of ultrasonic waves propagation between two media of different acoustic impedance, there is a phenomenon of mode conversion. So, it may be a great topic when using the same technique by taking into count other waves generated either by modes conversion or generated by the transducer such as shear wave.

We noticed that synthetic aperture focusing technique clearly indicate significant volumetric reflectors within the tested concrete, but because of the shadowing effects, other defects behind the first or damage may not be detected. So, it is also suggested to do deeper research for inspection in the case of parallel defects.

REFERENCES

[1] Jian-Hua TONG, Shu-Tao LIAO, "*Using the Synthetic Aperture Focusing Technique with Elastic Wave Method to detect the defects inside concrete structures*", 11th European Conference on Non-Destructive Testing (ECNDT 2014), October 6-10, 2014, Prague, Czech Republic.

[2] Martin Schickert, Martin Krause, and Wolfgang Muller *"Ultrasonic Imaging of Concrete Elements Using Reconstruction by Synthetic Aperture Focusing Technique"*, 10.1061/(ASCE)0899-1561(2003)15:3(235).

[3] Oscar Victor M. Antonio, Jr.and Sohichi Hirose, "*Ultrasonic Imaging of Concrete by Synthetic Aperture Focusing Technique Based on Hilbert-Huang Transform of Time Domain Data*", Materials Transactions, Vol. 53, No. 4 (2012) pp. 621 to 626.

[4] Lawrence Azar, *Ultrasonic Phased Arrays for the Condition Assessment of Concrete Structures*, Massachusetts Institute of Technology. May 1998.

[5] Abhijit Ganguli, Carey M.Rappaport, David Abramo, SaraWadia-Fascetti, "*Synthetic aperture imaging for flaw detection in a concrete medium "*, NDT&E International, 5 September, 2011.

[6] Xuefei Guan, Jingjing He, El Mahjoub Rasselkorde, "*A time-domain synthetic aperture ultrasound imaging method for material flaw quantification with validations on small-scale artificial and natural flaws*", Ultrasonic, 24 September 2014.

[7] Michele Carboni, Stefano Cantini, "*Advanced ultrasonic, ''Probability of Detection'' curves for designing in-service inspection intervals*", Intenational journal of fatigue, 15 July 2015.

[8] Chung-Yue Wang, Shu-Tao Liao, Jian-Hua Tong, Chin-Lung Chiu, "*Numerical and experimental study on multi-directional SAFT to detect defects inside plain or reinforced concrete*", construction and building materials, 9 December 2014.

[9] K. Nakahata, S.Tokumasu, A.Sakai, Y.Iwata, K.Ohira, Y.Ogura, "*Ultrasonic imaging using signal post-processing for a flexible array transducer* ", NDT&E International, 4 April 2016.

[10] Patrick Avanesians, Moe Momayez, "*Wave separation: Application for arrival time detection in ultrasonic signals*", Ultrasonics, 14 August 2014.

[11] Hajin Choi, *evaluation of internal damage in reinforced concrete elements using ultrasonic tomography*. A dissertation Submitted in partial fulfillment of the requirements for the degree of Doctor of Philosophy in Civil Engineering in the Graduate College of the University of Illinois at Urbana-Champaign, 2016.

[12] Ch. Trela, Th. Kind, M. Schubert, M. Gunther, *Detection of Weak Scatterers in Reinforced Concrete Structure*, BAM - Federal Institute for Materials Research and Testing Unter den Eichen 87, 12205, Berlin, Germany Christiane. Trela@bam.de. 15th International Conference on Ground Penetrating Radar - GPR 2014.

[13] Protected by U.S. Patents 7,519,518; 7,596,474; and 7,623,991. Patents pending. *Introduction to COMSOL Multiphysics.* 1998–2011 COMSOL. VERSION 4.2a.

[14] Moe Momayez, Zahra Hosseini, Ferri Hassani, and Daniel Lévesque, *detection of inclined cracks inside concrete structures by ultrasonic SAFT*, 2007 – Review of Progress in Quantitative NDE, Golden, Colorado, July 22 – July 27, 2007.

[15] Jing-Kui Zhang, Weizhong Yan, and De-Mi Cui, *Concrete Condition Assessment Using Impact-Echo Method and Extreme Learning Machines*; Published: 26 March 2016.

[16] S. Ashok Kumar and M. *Santhanam, Detection of Concrete Damage Using Ultrasonic Pulse Velocity Method*, Proc. National Seminar on Non-Destructive Evaluation Dec. 7 - 9, 2006, Hyderabad.

[17] G Karaiskos, A Deraemaeker, D G Aggelis and D Van Hemelrijck, *Monitoring of concrete structures using the ultrasonic pulse velocity method*. Smart Mater. Struct. 24 (2015) 113001 (18pp).

[18] Dalibor Sekulic, Irina Stipanovic, Emilija Barisic, *Damage Assessment of Concrete Column using Combination of Nondestructive Methods.* Civil Engineering Institute of Croatia, Department for Concrete and Masonry Structures J. Rakuse 1, 10000 Zagreb, Croatia, Europe, August 2008.

[19] G Karaiskos, A Deraemaeker, D G Aggelis and D Van Hemelrijck, *Monitoring of concrete structures using the ultrasonic pulse velocity method*. Smart Materials and Structures, 15 October 2015.

[20] Ahmad Zaki, Hwa Kian Chai , Dimitrios G. Aggelis and Ninel Alver, *Non-Destructive Evaluation for Corrosion Monitoring in Concrete: A Review and Capability of Acoustic Emission Technique*, Sensors 5 August 2015.

[21] Eunjong Ahn, Hyunjun Kim, Sung-Han Sim , Sung Woo Shin, and Myoungsu Shin, *Principles and Applications of Ultrasonic-Based Nondestructive Methods for Self-Healing in Cementitious Materials*, materials (MDPI) 10 March 2017.

[22] Robert Long, *the improvement of ultrasonic apparatus for the routine inspection of concrete, Imperial College of science, technology and medicine.* London SW7 2BX, 2000.

[23] Robyn T. Umeki, *Applying synthetic aperture, coded excitation, and tissue harmonic imaging techniques to allow ultrasound imaging with a virtual source*, Master of Science in Electrical and Computer Engineering in the Graduate College of the University of Illinois at Urbana-Champaign, 2011.

[24] Snowdon, Paul C., *Investigation into the use of zero angle ultrasonic probe array for defect detection and location*, Durham theses, Durham University. Available at Durham E-Theses Online: http://etheses.dur.ac.uk/2283/, 2007.

[25] Tadeusz Stepinski, *Synthetic Aperture Focusing Technique in Ultrasonic Inspection of Coarse Grained Materials*, Uppsala Universitet, Signals and Systems Box 528 SE-751 20 Uppsala Sweden, SKI December 2007.

[26] Dwight Clayton, Hector Santos-Villalobos, Justin Baba, *evaluation of advanced signal processing techniques to improve detection and identification of embedded defects*, Oak Ridge National Laboratory, September 2016.

[27] Martin Krause, Ulrike Dackermann, Jianchun Li, *Elastic wave modes for the assessment of structural timber: Ultrasonic echo for building elements and guided waves for pole and pile structures*,

[28] Klaus MAYER, Mohamad IBRAHIM, Martin KRAUSE, Marcus SCHUBERT, *Requirements for a Small Size Ultrasonic Imaging System for Inspection of Concrete Elements*, 19th World Conference on Non-Destructive Testing 2016.

[29] Samson Hansen Sackey, Samuel Nartey Kofie, and Abdul Karim Armah, "A Randomized Approach to Sparse Subspace Clustering using Spectl clustering," International Research Journal of Advanced Engineering and Science, Volume 4, Issue 3, pp. 276-280, 2019.